Semimicroscopic algebraic study of the α-cluster states of the ^{18}O nucleus

G. Lévai,[1,2,*] J. Cseh,[1,2,*] and W. Scheid[1]
[1]*Institut für Theoretische Physik der Justus-Liebig-Universität, D-6300 Giessen, Germany*
[2]*Institute of Nuclear Research of the Hungarian Academy of Sciences (ATOMKI), H-4001 Debrecen, Hungary*
(Received 28 April 1992)

The ^{14}C+α system is described in terms of the new semimicroscopic algebraic cluster model, which is based on the coupling of the SU(3) shell model to the vibron model. Molecular states of the ^{18}O nucleus built on the ^{14}C levels with (0,2) SU(3) quantum numbers are constructed, and the corresponding energy eigenvalues are obtained from a model Hamiltonian with SU(3) dynamical symmetry. The model is able to account for 34 experimental ^{18}O states assigned to even- or odd-parity bands, some of which are new. Enhanced $E1$ and $E2$ transitions are also obtained.

PACS number(s): 21.60.Fw, 21.60.Gx, 27.20.+n

I. INTRODUCTION

Following some early studies on ^{18}O [1–4], much experimental and theoretical attention was concentrated on this nucleus when enhanced $E1$ transitions were predicted [5–7] as a signature of the dipole degrees of freedom related to its ^{14}C+α cluster structure. According to this scenario, $E1$ transitions originate from the asymmetry of the center of charge and center of mass in systems where the charge-to-mass ratio is different for the two clusters. This prediction for the ^{18}O was confirmed experimentally [8], initiating further theoretical studies of the ^{14}C+α system. The interpretation of the results, however, was not unequivocal. Some of the studies [9,10] supported the idea of the existence of a mixed parity dipole band consisting of the ^{18}O states 0^+(3.63 MeV), 1^-(4.46), 2^+(5.26), 3^-(8.28), and (probably) 4^+(10.29) implied by the phenomenologic dipole picture [5,11], while some others did not. A generator-coordinate method (GCM) calculation first assuming only the $^{14}C_{g.s.}+\alpha$ configuration [12], then considering the $^{14}C(2_1^+)+\alpha$ channel as well [13], gave bands with unique parity. At about the same time a coupled-channel orthogonality condition model (CCOCM) calculation including the same two ^{14}C states was also performed [14]. This latter study also yielded separated positive- and negative-parity bands.

Here we apply the new semimicroscopic algebraic cluster model [15,16] to the α-cluster states of the ^{18}O nucleus. In this model the internal cluster structure is described in terms of the SU(3) shell model [17], while the relative motion is treated within the vibron model [5,11]. The model space is constructed to be free from the Pauli-forbidden states and from the spurious excitations of the center-of-mass motion. In this respect it is similar to the microscopic SU(3) cluster model. The interactions, however, are handled phenomenologically, and in this respect the model is similar to the algebraic models of various collective motions.

By applying this model to the ^{14}C+α system we address the question, whether the algebraic model is able to reproduce the whole energy spectrum of ^{18}O together with the enhanced electric dipole and quadrupole transitions [18,19] when we combine the dipole degrees of freedom of the relative motion with the internal degrees of freedom of the nonmagic ^{14}C core. Our choice is also motivated by the fact that a wide variety of models (both microscopic and phenomenologic) have been used earlier for the description of the ^{18}O nucleus assuming a ^{14}C+α configuration, and we expect that comparing our results with other calculations can show how well microscopic effects are approximated by the present semimicroscopic model. Furthermore, the amount of experimental information (on the energy levels and the electromagnetic transitions) has increased considerably in the past couple of years [18,19], so we can rely on a more complete data set than what has been considered in earlier theoretical studies.

The arrangement of the paper is as follows. In Sec. II we give a brief review of the model we apply. Section III contains the results, such as the form of the wave functions, the energy spectrum, and electromagnetic transitions derived from the model in the SU(3) dynamical symmetry approximation. Finally, we summarize the results in Sec. IV.

II. THE MODEL

In the semimicroscopic algebraic model of a core-plus-alpha-particle system [15,16] the internal structure of the core (C) is taken into account by allowing a set of SU(3) shell model states characterized by the following group chain, and labeled by the corresponding irreducible representations [17,20]:

*Permanent address: Institute of Nuclear Research of the Hungarian Academy of Sciences (ATOMKI), H-4001 Debrecen, Hungary.

$$\begin{array}{ccccccc} U_C^{ST}(4) & \otimes & U_C(3) & \supset & U_C^S(2)\otimes U_C^T(4)\otimes & O_C(3) & \\ |[f_1^C,f_2^C,f_3^C,f_4^C], & & [n_1^C,n_2^C,n_3^C], & & S_C, \quad T_C, & K_C,L_C\rangle\ . & \end{array} \tag{1}$$

$U_C^{ST}(4)$ is the spin-isospin group of Wigner [21] which, due to the total antisymmetry of the cluster wave function is also uniquely related to the permutational symmetry of the nucleons. $U_C(3)$ is the orbital group, the irreducible representations $[n_1^C,n_2^C,n_3^C]$ which characterize the distribution of oscillator quanta (carried by the nucleons) in the three spatial directions, while S_C and T_C denote the spin and isospin of the core. L_C is the angular momentum assigned to the orbital part of the core wave function, while the role of K_C is to distinguish between states with the same L_C within an $U_C(3)$ multiplet.

The relative motion (R) of the clusters is described by the U(3) limit of the vibron model corresponding to the group chain [11]

$$\begin{array}{cccc} U_R(4) & \supset & U_R(3) & \supset O_R(3) \\ |[N,0,0,0], & & [n_\pi,0,0], & L_R\rangle\ . \end{array} \tag{2}$$

Here n_π is the number of dipole bosons (π bosons), characterizing the excitations of the relative motion of the α particle and the core. Its possible values are limited from above by $N=n_\pi+n_\sigma$, where N is the number of dipole and monopole bosons together, while a lower limit also follows from the Pauli principle [22,23]. According to this, n_π should not be smaller than the number of oscillator quanta carried by the nucleons of the smaller cluster (α) if we view the unified nucleus as a whole, in its ground state. Finally, L_R is the orbital angular momentum assigned to the relative motion of the clusters.

Similarly to other algebraic models of coupled degrees of freedom, the two group chains are coupled. Now this is done on the level of the U(3) groups, resulting group chain (3), which supplies quantum numbers to label the model states:

$$\begin{array}{ccccccccc} U_C^{ST}(4) & \otimes & U_C(3) & \otimes & U_R(4) & \supset U_C^S(2)\otimes U_C^T(4)\otimes U_C(3)\otimes & & U_R(3) & \\ |[f_1^C,f_2^C,f_3^C,f_4^C], & & [n_1^C,n_2^C,n_3^C], & & [N,0,0,0], & S_C, \quad T_C, & & [n_\pi,0,0] & \end{array}$$

$$\begin{array}{cccccc} \supset U(3) & \otimes U_C^S(2)\otimes U_C^T(2) & \supset O(3) & \otimes SU_C^S(2)\otimes SU_C^T(2) & \supset SU(2) & \otimes SU_C^T(2) \\ [n_1,n_2,n_3], & \chi,L, & & & J\rangle. & \end{array} \tag{3}$$

Instead of the U(3) groups closely related to the graphic oscillator picture, practical calculations make more extensive use of SU(3) groups. SU(3) representations labeled by (λ,μ) can be readily derived from the $[n_1,n_2,n_3]$ U(3) ones by setting $\lambda=n_1-n_2$ and $\mu=n_2-n_3$. From now on we restrict the formalism to the SU(3) notation. χ is a quantum number used in the $SU(3)\supset O(3)$ [or $U(3)\supset O(3)$] decomposition [24] to identify states with the same O(3) representation within an SU(3) one. It is defined similarly to the quantum number K of the Elliott $SU(3)\supset O(3)$ basis [17,20], with the difference that the latter basis is not orthonormal. χ also differs slightly from the κ quantum number of the orthonormal Vergados basis [25] in the way of handling certain states with high angular momenta. The spin J of the general basis state is obtained from angular momentum coupling of L and S_C. The parity is determined by the parity assigned to the relative motion $[(-1)^{n_\pi}]$ and to the core nucleus $[(-1)^{n_1^C+n_2^C+n_3^C}]$. These labels, together with the T_C isospin of the core, supply a complete set of quantum numbers to label the basis states as follows:

$$|[f_1^C,f_2^C,f_3^C,f_4^C](\lambda_C,\mu_C)S_CT_C,Nn_\pi;(\lambda,\mu)\chi LJ^\pi M\rangle. \tag{4}$$

Some of these basis states are Pauli forbidden, or correspond to spurious center-of-mass motion of the unified nucleus. A simple procedure for excluding these states on the basis of a matching condition between the antisymmetric shell model basis and the cluster model basis in Eq. (4) is given in Refs. [15,16]. Since the spin-isospin symmetry is not affected by the α particle, this means the exclusion of states with specific (λ,μ) labels.

In principle, several internal core configurations can be allowed, nevertheless usually it is enough to consider only a single $SU_C(3)$ multiplet, the one assigned to the ground state. The particular choice of the core nucleus usually also selects certain spin-isospin configurations.

In contrast to the microscopic basis, physical operators are treated phenomenologically, reflecting the semimicroscopic nature of the model. In particular, they are constructed as Hermitian combinations of the group generators. Like the wave functions, these operators can also be characterized by irreducible representations of the groups in group chain (3). These algebraic manipulations simplify the calculations to a considerable extent: for example, an analytic solution of the eigenvalue problem is possible if dynamical symmetry holds, i.e., if the Hamiltonian is built up from the invariants of group chain (3). In general the Hamiltonian has to be diagonalized, nevertheless the evaluation of matrix elements is helped significantly by tensor algebra in this case too.

Similarly to other algebraic models the Hamiltonian usually contains terms which are linear or quadratic ex-

pressions of the group generators, but higher-order terms can also be used if required. An important new element here is that due to the presence of the $U_C^{ST}(4)$ and $U_C^T(2)$ groups, the Hamiltonian can have isospin-dependent terms as well. The parameters of the various terms in the Hamiltonian are fixed by fitting the model spectrum to the experimental one. One can also include higher (second- or third-order) terms in the phenomenologic electromagnetic transition operators in order to describe a wide enough range of transitions. These terms are particularly important in calculations within the dynamical symmetry limit, when the basis states are not mixed and the lowest-order transition operators, several of which are group generators, are able to connect model states only in a limited domain. Reduced transition probabilities with multipolarity ωl are calculated from the matrix elements of the corresponding transition operator $T^{(\omega l)}$ in the usual way:

$$B(\omega l;\alpha_i J_i \rightarrow \alpha_f J_f)=\frac{1}{2J_i+1}|\langle \alpha_f J_f \| T^{(\omega l)} \| \alpha_i J_i \rangle|^2 . \quad (5)$$

The parameters of the phenomenologic transition operator $T^{(\omega l)}$ are fitted to the experimental data, usually by requiring the reproduction of some precisely known $B(\omega l)$ values. Cluster spectroscopic factors can also be calculated in terms of the algebraic approach [26].

III. RESULTS FOR THE ^{18}O NUCLEUS IN THE SU(3) DYNAMICAL SYMMETRY APPROXIMATION

A. The model states

We assume that in the ground state of the ^{14}C nucleus the 14 nucleons occupy the s and p shell according to the [4,4,4,2] permutational symmetry, which means that the distribution of the oscillator quanta (carried by the ten nucleons on the p shell) corresponds to the $[n_2^C,n_2^C,n_3^C]=[4,4,2]$ $U_C(3)$ representation. Furthermore, due to the antisymmetry of the wave function, the irreducible representation of the $U_C^{ST}(4)$ spin-isospin group must have a Young pattern adjoint to that of the permutational symmetry group (S_{14}) [17,20], therefore we have $[f_1^C,f_2^C,f_3^C,f_4^C]=[4,4,3,3]$. These are two spin-isospin configurations belonging to this $U_C^{ST}(4)$ representation, one with $T_C=1$ and $S_C=0$, the other with $T_C=0$ and $S_C=1$, but the latter one is obviously irrelevant to the ^{14}C case with $T_{Cz}=1$. The orbital part of the core wave function is characterized by the $(\lambda_C,\mu_C)=(0,2)$ $SU_C(3)$ representation containing two states with $L_C=0$ and $L_C=2$, which, due to $S_C=0$ represent the full angular momentum of the core states in this configuration. Thus, in addition to the ground state of the ^{14}C nucleus (with $J_C^\pi=0^+$ and $T_C=1$,) we also include the first $J_C^\pi=2^+$ state at $E_x=7.012$ MeV (also with $T_C=1$) in our model calculations. It has to be mentioned that there are several other ^{14}C somewhat below $E_x=7$ MeV; nevertheless, the coupling of these states to the ground state is less significant than that of the $2^+(7.01$ MeV) state.

The excitations of the relative motion of the ^{14}C and α clusters are characterized by n_π. According to the model its lowest possible value is $n_{\pi_{\min}}=6$, while its upper limit is given by N. The choice of N is a technical question rather than a physical one: its role is to provide a large enough model space to account for the experimental data. It appears explicitly in some matrix elements, influencing slightly the relative strength of electromagnetic transitions between different major shells. In our calculations we used $N=12$.

Following the notations of Eq. (4) the general form of the model states is

$$|[4,4,3,3](0,2)S_C=0T_C=1,Nn_\pi;(\lambda,\mu)\chi L^\pi=J^\pi M\rangle , \quad (6)$$

where, due to $S_C=0$, J and L have the same values, so we shall omit one of them (L) as a redundant label. (λ,μ) is obtained from the $(0,2)\otimes(n_\pi,0)$ outer product, and its possible values are $(\lambda,\mu)=(n_\pi,2)$, $(n_\pi-1,1)$, and $(n_\pi-2,0)$. According to the matching condition between the states (6) and the SU(3) shell model basis for the unified ^{18}O nucleus, some of the states [SU(3) multiplets (λ,μ)] have to be excluded from the lowest two allowed major shells (with $n_\pi=6$ and 7). Our model states with $n_\pi\leq 9$ are presented in Table I, where we used only the essential quantum numbers for labeling. We mention here that our basis is practically the same as the one used by Suzuki *et al.* [14] in a coupled-channel orthogonality condition model (CCOCM) calculation, and which was obtained by evaluating the norm kernel of the resonating group method (RGM). The only difference arises from the finiteness of the vibron model basis due to the finite number of bosons (N).

The explicit form of the wave functions in the SU(3) coupled basis can be written in terms of Clebsch-Gordan coefficients and $SU(3)\supset O(3)$ isoscalar factors [24,25]:

$$|[4,4,3,3](0,2)S_C=0T_C=1,Nn_\pi;(\lambda,\mu)\chi J^\pi M\rangle = \sum_{L_C L_R}\langle (0,2)L_C;(n_\pi,0)L_R\|(\lambda,\mu)\chi J\rangle \sum_{M_C M_R}\langle L_C M_C L_R M_R|JM\rangle \times|[4,4,3,3](0,2)L_C S_C=0M_C T_C\rangle|N(n_\pi,0)L_R M_R\rangle . \quad (7)$$

The parity of the states is determined uniquely by n_π, so we did not write it out explicitly on the right-hand side (r.h.s.) of Eq. (7). The phenomenologic operators act either on the coupled wave function [as in the l.h.s. of Eq. (7)], or on its core (C), or relative motion (R) component (in the r.h.s.). A summary of the algebraic techniques used in the computation of matrix elements in an SU(3) coupled basis can be found in the appendix of Ref. [27].

TABLE I. Pauli-allowed model states for the $^{14}C+\alpha$ system with $n_\pi \leq 9$.

n_π	(λ,μ)	χ^π	J^π
6	(4,0)	0^+	$0^+2^+4^+$
7	(5,0)	0^-	$1^-3^-5^-$
7	(6,1)	1^-	$1^-2^-3^-4^-5^-6^-7^-$
8	(6,0)	0^+	$0^+2^+4^+6^+$
8	(7,1)	1^+	$1^+2^+3^+4^+5^+6^+7^+8^+$
8	(8,2)	0^+	$0^+2^+4^+6^+8^+$
8	(8,2)	2^+	$2^+3^+4^+5^+6^+7^+8^+9^+10^+$
9	(7,0)	0^-	$1^-3^-5^-7^-$
9	(8,1)	1^-	$1^-2^-3^-4^-5^-6^-7^-8^-9^-$
9	(9,2)	0^-	$1^-3^-5^-7^-9^-$
9	(9,2)	2^-	$2^-3^-4^-5^-6^-7^-8^-9^-10^-11^-$

As it can be seen from Eq. (7), the wave functions in general have components from both internal ^{14}C states (except for the unnatural parity ones, or those with $J > n_\pi$). The ratio of the $L_C=0$ and $L_C=2$ components is determined by the isoscalar factors. As we can expect from the statistical weight of the $L_C=0$ and 2 states, the latter one dominates the majority of the basis states. The only exceptions are states with $(\lambda,\mu)\chi=(n_\pi,2)0$, most of which have a 50 to 75% contribution from the $L_C=0$ configuration. Besides these states, some other states with high angular momenta also have a more balanced share of the two internal ^{14}C states due to the general trend that mixing increases with increasing J.

B. The energy spectrum

We restricted our calculations to the SU(3) dynamical symmetry of the model, so the Hamiltonian was constructed from invariants of the groups in group chain (3). As a result of this, the Hamiltonian is diagonal in basis (6), and the energy eigenvalues can be obtained as closed expressions of the quantum numbers n_π (λ,μ), χ, and J. Since all model states have the same isospin ($T=1$), we do not consider isospin-dependent terms in the Hamiltonian.

In order to fix the model parameters we tried to identify rotational bands with levels roughly following an $E \simeq J(J+1)$ spacing in the experimental energy spectrum [18]. Several bands were identified in this way, partly in agreement with the band assignment of other models [2,13,14]. The J^π content of our model basis (in Table I) agreed surprisingly well with the experimental data set consisting of states with definite or tentative J^π assignment. Taking only states with $T=1$ below $E_x=10$ MeV, for example, we could assign model correspondents to the vast majority of experimental states. Among the 22 states with definite J^π value in this region there was only a single 0^- state (at $E_x=6.880$ MeV) which was unaccounted for by our model. Based on these initial results we (more or less speculatively) identified other experimental states, at higher energy or with tentative J^π assignment, with model states, and determined the final model spectrum by a weighted least-squares fit of the model parameters. The weight of each state was $W=1/E_{x,\mathrm{exp}}$ (MeV), except for the ground state where we used $W=1$. This W was halved for states with uncertain J^π assignments. We present the resulting energy spectrum in Figs. 1 and 2, respectively.

We used the following seven-parameter expression for the energy in the fitting procedure:

$$E=\epsilon+\nu(-1)^{n_\pi}+\gamma n_\pi+\eta C_2(\lambda,\mu)+\sigma C_3(\lambda,\mu) + \xi\chi^2+\beta J(J+1) . \quad (8)$$

The resulting parameter set (in units of MeV) was $\epsilon=-12.817$, $\nu=-0.946$, $\gamma=1.570$, $\eta=0.332$, $\sigma=-0.015$, $\xi=-0.817$, and $\beta=0.183$. Expression (8) is essentially an anharmonic oscillator spectrum distorted by various interactions. Instead of the usual quadratic term in n_π, now the $(-1)^{n_\pi}$ term proved more useful: its role was to separate the positive and negative parity part of the spectrum. n_π represents the harmonic oscillator term, while $C_2(\lambda,\mu)=\lambda^2+\mu^2+\lambda\mu+3\lambda+3\mu$ and $C_3(\lambda,\mu)=(\lambda-\mu)(\lambda+2\mu+3)(2\lambda+\mu+3)$ are the eigenvalues of the second- and third-order Casimir invariants of the SU(3) group for the representation (λ,μ). As phenomenologic interaction terms in the Hamiltonian, $C_2(\lambda,\mu)$ and $C_3(\lambda,\mu)$ can be expressed in terms of the SU(3) generators, i.e., the $Q^{(2)}$ quadrupole and the $L^{(1)}$ angular momentum operators in the following way (see, for example, Ref. [28]):

$$C_2(\mathrm{SU}(3))=\tfrac{1}{6}Q^{(2)}\cdot Q^{(2)}+\tfrac{1}{2}L^{(1)}\cdot L^{(1)} , \quad (9a)$$

$$C_3(\mathrm{SU}(3))=-\frac{1}{36}\left[\frac{7}{2}\right]^{1/2}[Q^{(2)}\times Q^{(2)}]^{(2)}\cdot Q^{(2)} + \frac{1}{4}\left[\frac{5}{2}\right]^{1/2}[L^{(1)}\times Q^{(2)}]^{(1)}\cdot L^{(1)} . \quad (9b)$$

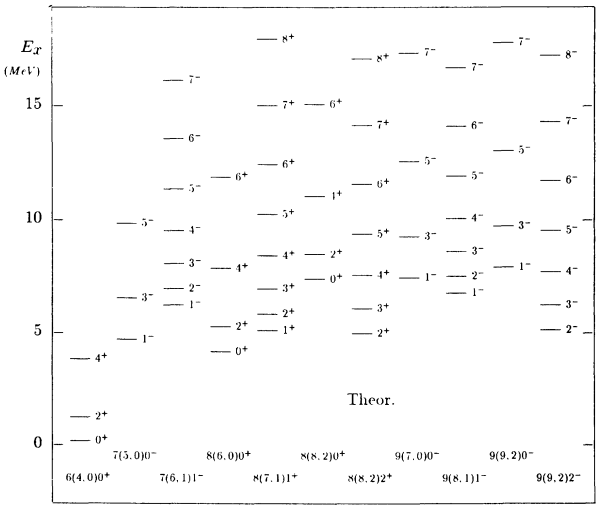

FIG. 1. The energy spectrum of the $^{14}C+\alpha$ system obtained from the SU(3) dynamical symmetry limit of the semimicroscopic algebraic cluster model. The cluster bands are labeled by the symbols $n_\pi(\lambda,\mu)\chi^\pi$.

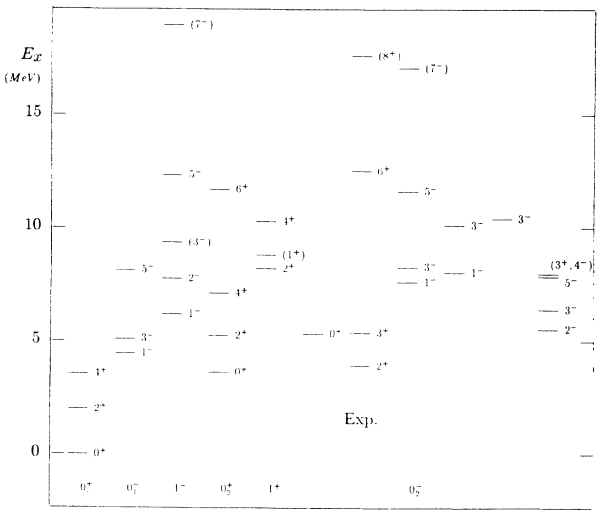

FIG. 2. The experimental energy spectrum of the ^{18}O nucleus [18] arranged into bands suggested by the model calculations. Notations (K^π) used earlier for labeling some of the bands are also shown.

Here $A^{(k)}\cdot B^{(k)}$ is the scalar product of two rank-k spherical tensors, while $[A^{(j)}\times B^{(k)}]^{(l)}$ is the tensorial product of a rank-j and a rank-k tensor resulting a rank-l spherical tensor. The numerical factors in (9a) and (9b) may depend on the conventions accepted.

The term proportional to $J(J+1)$ in Eq. (8) is the rotational energy obtained as the eigenvalue of the $J^{(1)}\cdot J^{(1)}$ angular momentum square operator in a state with angular momentum J. Here we again stress that L and J have equal values, and therefore the effect of $C_2(\mathrm{O}(3))=L^{(1)}\cdot L^{(1)}$ is the same as that of $C_2(\mathrm{SU}(2))=J^{(1)}\cdot J^{(1)}$, hence we include only one of these operators in the Hamiltonian. The energy proportional to χ^2 is a phenomenological term which splits the different χ bands within an SU(3) representation. Just like the other terms in Eq. (8), it is included here as a phenomenologic interaction, which is diagonal in the SU(3) basis. It is worth mentioning, however, that a similar interaction has been introduced recently in the shell model description [29]. This operator was constructed from SU(3) generators and was found to be nearly diagonal in the Elliott basis [17].

The experimental energy spectrum in Fig. 2 consists of 28 states with definite, and 6 states with uncertain J^π. The states missing from some of the bands are mainly unnatural parity ones or are expected at higher energy. In addition to the 0^- state mentioned before, there are only two more states with tentative J^π assignment below $E_x=10$ MeV to which we cannot associate theoretical states. One is a (2^-) state at $E_x=6.351$ MeV, and the other is a (3^-) state at $E_x=9.672$ MeV. Besides these, there are ten more experimental levels between $E_x=8.4$ MeV and 10 MeV with unknown J^π. These could account for several theoretical states in Fig. 1. There are many more states above 10 MeV with or without J^π assignment, but we did not analyze them in terms of our model. Some experimental states with even parity around $E_x=12$ MeV and some odd-parity ones around $E_x=14$ MeV can be interpreted, however, as the lowest-lying states with $n_\pi=10$ and 11, respectively.

Some of the 11 cluster bands in Figs. 1 and 2 are similar to certain bands discussed in other studies. The $n_\pi(\lambda,\mu)\chi^\pi=8(6,0)0^+$ band, for example, consists of the same experimental levels as the $^{14}\mathrm{C}+\alpha$ band of Buck *et al.* [2], derived from a local potential cluster model, or as the "α-transfer band" of Suzuki *et al.* [14], interpreted in terms of a coupled-channel orthogonality condition model calculation. In this latter study the ground-state band and the negative-parity "partner" of the α-transfer band was also reproduced. In our approach these bands are labeled as $n_\pi(\lambda,\mu)\chi^\pi=6(4,0)0^+$ and $7(5,0)0^-$, respectively. It was also suggested [14] that the α-transfer band and its negative parity partner are analogous to the $K^\pi=0^+$ and 0^- bands based on the $0^+(6.05$ MeV) and $1^-(9.63$ MeV) states of the ^{16}O nucleus. Furthermore, the similarity between some cluster bands of nuclei with $A=16,18,19$, and 20 was also discussed [30]. In addition to the examples mentioned above, three more bands were analyzed in Ref. [13] in terms of a microscopic cluster study. These authors use the same two ^{14}C states in the generator coordinate formalism and get also the $K^\pi=1^+$, 0_2^-, and 1^- bands, corresponding (up to some minor exceptions) to our $n_\pi(\lambda,\mu)\chi^\pi=8(7,1)1^+$, $9(7,0)0^-$, and $7(6,1)^-$ bands, respectively. The remaining five bands in Fig. 1 including the low-lying $\chi^\pi=2^+$ and 2^- bands were not found in these earlier studies. The $2^+(3.92$ MeV) and $0^+(5.34$ MeV) states, which we assigned to the $n_\pi(\lambda,\mu)\chi^\pi=8(8,2)2^+$ and 0^+ bands, are considered in Refs. [3,14] to have a dominantly shell model structure.

Referring in advance to the next section, we mention here that the five members of the mixed parity "dipole molecular band" discussed by several authors [9,8,10,19] belong to four different bands in our approach. Three of these, the $n_\pi(\lambda,\mu)\chi^\pi=7(5,0)0^-$, $8(6,0)0^+$, and $9(7,0)0^-$ bands, seem to consist of states usually considered to have well-developed cluster character, including the first four members of the dipole band.

In summary, our model is able to reproduce a more complete ^{18}O spectrum than other model calculations known to us [2–4,13,14]. This is partly due to the recent extension of experimental information [18], which allowed us to include certain previously unknown or misinterpreted ^{18}O levels in our work.

C. Electromagnetic transitions

A relatively large experimental data set of electromagnetic transitions between ^{18}O states is available [18], partly extended by a recent experiment [19]. Here we present reduced $E2$ and $E1$ transition probabilities obtained from our model and compare them with the experimental values, as well with the results of some other model calculations [3,14,13] assuming a $^{14}\mathrm{C}+\alpha$ configuration of the ^{18}O nucleus.

1. E2 transitions

The following phenomenological electric quadrupole transition operator is considered:

$$T_m^{(E2)}=q_R Q_{Rm}^{(2)}+q_C Q_{Cm}^{(2)}+p_R P_{Rm}^{(2)} . \quad (10)$$

The $Q_R^{(2)}$ and $Q_C^{(2)}$ quadrupole momentum operators, which are $SU_R(3)$ and $SU_C(3)$ generators, respectively, act on the relative and the core component of the wave function in Eq. (7). Their selection rules are $\Delta n_\pi=0$, $\Delta\lambda=\pm1$, $\Delta\mu=\pm1$, so they allow interband transitions as well, which are usually much weaker than the intraband ones, and vanish if $q_R=q_C$ holds. (All the signs in the selection rules should be taken either in lower or upper case.) The operator $P_R^{(2)}=[[\sigma^\dagger\times\tilde{\pi}]^{(1)}\times[\sigma^\dagger\times\tilde{\pi}]^{(1)}]^{(2)}+\text{H.c.}$ introduced earlier in the vibron-fermion model [27,31] is able to generate transitions between major shells. It allows relatively strong transitions with $\Delta n_\pi=\pm2$, $\Delta\lambda=\pm2$, $\Delta\mu=0$ and somewhat weaker ones with $\Delta n_\pi=\pm2$, $\Delta\lambda=\pm1$, $\Delta\mu=\mp1$.

Experimental and theoretical reduced $E2$ probabilities are shown in Table II, together with the results from three other model calculations. These are two microscopic cluster studies [3,13] and a coupled-channel orthogonality condition model calculation [14]. In order to illustrate the selection rules of the operators in Eq. (10), we also show the quantum numbers assigned to the ^{18}O states in our model. Experimental data are from Refs. [19] and [18].

We used the most precisely determined even $\rightarrow$ even and odd $\rightarrow$ odd transitions with $\Delta n_\pi=0$ to fix q_R and q_C, while p_R was fitted independently to the $\Delta n_\pi=-2$

TABLE II. Reduced $E2$ transition probabilities (in W.u.) between ^{18}O states. The more recent experimental compilation in Ref. [19] was used, whenever it was possible. Otherwise data were taken from Ref. [18], as indicated below. (E_x is given in units of MeV.)

Experimental data			$B(E2)$theory			Present work		
$J_i^\pi(E_{xi})$	$J_f^\pi(E_{xf})$	$B(E2)_{\text{exp}}$	[13]	[14]	[3]	$B(E2)$	$n_\pi(\lambda,\mu)\chi$; $i\rightarrow f$	
$2^+(1.98)$	$0^+(0.0)$	3.4±0.1	2.9	8	2.38	3.4[b]	6(4,0)0	6(4,0)0
$4^+(3.55)$	$2^+(1.98)$	1.2±0.1	2.1	2.2	1.26	3.1		6(4,0)0
$3^-(5.10)$	$1^-(4.46)$	<57	11	28		6.9	7(5,0)0	7(5,0)0
$5^-(8.13)$	$3^-(5.10)$	5±5[a]	8	29		5.0[b]		7(5,0)0
$1^-(6.20)$	$3^-(5.10)$	<166				1.5	7(6,1)1	7(5,0)0
$2^-(7.77)$	$1^-(4.46)$		2			2.2		7(5,0)0
	$3^-(5.10)$		5			3.9		7(5,0)0
	$1^-(6.20)$		7			15.8		7(6,1)0
	$3^-(8.28)$		2			0.4		9(7,0)0
$0^+(3.63)$	$2^+(1.98)$	17±2	4.3	15	6.23	3.8	8(6,0)0	6(4,0)0
$2^+(5.26)$	$0^+(0.0)$	2.0±0.1	1.6	2.0	1.61	2.0[b]		6(4,0)0
	$2^+(1.98)$	0.9±0.5	1.5	3.7	1.39	1.6		6(4,0)0
	$4^+(3.55)$	20.3±10.8	0.7	5.2		0.7		6(4,0)0
	$0^+(3.63)$	23±14	24	17	31.8	9.4		8(6,0)0
	$2^+(3.92)$				6.13	0		8(8,2)2
$4^+(7.12)$	$2^+(1.98)$	3.3±0.8	2.3	13	1.86	4.5		6(4,0)0
	$4^+(3.55)$	<0.15	0.6	3.5	0.73	0.9		6(4,0)0
	$2^+(5.26)$	<12	32	17	37.5	10.9		8(6,0)0
	$2^+(3.92)$	2.3±0.6			4.02	0		8(8,2)2
$6^+(11.69)$	$4^+(3.55)$		1.3			7.1		6(4,0)0
	$4^+(7.12)$			30		7.1		8(6,0)0
$2^+(8.21)$	$0^+(0.0)$	0.9±0.3[a]	0.06			0	8(7,1)1	6(4,0)0
	$2^+(1.98)$		0.18			0		6(4,0)0
	$4^+(3.55)$	2.4±1.0[a]	0.16			0		6(4,0)0
	$(1^+)(3.55)$		18			89.1		8(7,1)1
$4^+(10.29)$	$2^+(1.98)$		0.14			0		6(4,0)0
	$4^+(3.55)$		0.09			0		6(4,0)0
	$2^+(5.26)$		5.2	2.5		8.2		8(6,0)0
	$2^+(8.21)$		29			45.9		8(7,1)0
$0^+(5.34)$	$2^+(1.98)$	1.5±0.5			0.29	0	8(8,2)0	6(4,0)0
	$2^+(3.92)$	<15.0			0.45	92.7		8(8,2)2
$2^+(3.92)$	$0^+(0.0)$	1.5±0.2			0.28	0	8(8,2)2	6(4,0)0
	$2^+(1.98)$	5.6±3.7			1.32	0		6(4,0)0
$6^+(12.53)$	$4^+(10.29)$		30	29		4.0		8(7,1)1
$1^-(7.62)$	$1^-(4.46)$	$M1+E2$[a]				2.2	9(7,0)0	7(5,0)0
$3^-(8.28)$	$1^-(4.46)$	8±8[a]	13	9.8		2.6		7(5,0)0
	$3^-(5.10)$		4			1.2		7(5,0)0
$5^-(11.62)$	$3^-(8.28)$			41		15.4		9(7,0)0
$3^-(6.40)$	$1^-(4.46)$	9.7±6.0				0	9(9,2)2	7(5,0)0

[a]From Ref. [18].
[b]Used to fit model parameters.

transition with the smallest relative error. The numerical values of the parameters obtained in this way are $q_R=2.08$, $q_C=5.52$, and $p_R=0.07$.

The strongest transitions calculated from the semimicroscopic algebraic cluster model are the intraband ones. There are only two cases where predicted intraband transitions can be compared with experimental data. Although the prediction of our model for $B(E2;2^+(5.26)\rightarrow 0^+(3.63))$ is less than half of the mean experimental value, the two results are still in agreement due to the large experimental error bars. The very strong transitions within the SU(3) multiplets with $\mu=1$ and 2 arise because these transitions are much more sensitive to the asymmetry of the q_R and q_C parameters than those within the $(\lambda,0)$ bands, including the two transitions used in fixing the model parameters. By taking a more balanced parameter pair, e.g., $q_R=1.5$ and $q_C=2.9$ these large $B(E2)$ values could be halved, without changing the transition probabilities within $\chi=0$ bands by more than 10 to 20%. This latter parameter pair would result in the same $B(E2)$ value for the $2^+(1.98)\rightarrow 0^+(0.0)$ transition as the old one, and would yield $B(E2;5^-(8.13)\rightarrow 3^-(5.10))=4.4$ W.u. in satisfactory agreement with the experimental counterpart $B(E2)=5\pm 5$ W.u.

Transitions with $\Delta n_\pi=\pm 2$ in our model are reproduced fairly well. The only striking exceptions are the $0^+(3.63)\rightarrow 2^+(1.98)$ and $2^+(5.26)\rightarrow 4^+(3.55)$ transitions between the first two $\chi^\pi=0^+$ bands, but these large $B(E2)$ values are unexplained by the microscopic models as well [3,13]. There are some weak transitions which are forbidden in our model due to the selection rules of the phenomenological transition operators. The corresponding $B(E2)$ values are extremely small in the other models too [see, e.g., transitions to the ground-state band from the $n_\pi(\lambda,\mu)=8(7,1)$ and $8(8,2)$ states]. This seems to indicate that the SU(3) dynamical symmetry is a relatively good approximation of the real physical situation in this case.

An especially remarkable finding is that our results show a relatively strong correlation with the GCM results of Descouvemont and Baye [13], sometimes even in contradiction to the experimental data. This appears to indicate that the effects of antisymmetrization are fairly well approximated within the semimicroscopic algebraic cluster model. Our data show a less pronounced correlation with the results of another microscopic study [3] and are generally smaller than the $B(E2)$ values of the CCOCM calculation [14].

Quadrupole moments can also be computed using the phenomenological operator in Eq. (10) as

$$Q(\alpha,J)=\left[\frac{16\pi}{5}\right]^{1/2}\langle \alpha JM=J|T_0^{(E2)}|\alpha JM=J\rangle \ . \qquad (11)$$

Only the first two terms of $T^{(E2)}$ contribute to this expression. Using q_R and q_C fixed earlier, we find that the quadrupole momentum of the first excited state is -6.50 e fm^2, which agrees excellently with the larger of the two possible experimental values (-5.8 ± 1.5 e fm^2) presented in Ref. [18]. We remark here that the intrinsic quadrupole momentum (Q_0) in a band K^π defined [32] by

$$Q=Q_0\frac{3K^2-J(J+1)}{(J+1)(2J+3)} \qquad (12)$$

is constant by construction for states with $\mu=0$ in our model. The constant value of Q_0 for the members of a band suggests the rotational character of that particular band, therefore the $n_\pi(\lambda,\mu)\chi^\pi=6(4,0)0^+$, $7(5,0)0^-$, $8(6,0)0^+$, and $9(7,0)0^-$ bands in Fig. 1 are ideal rotational bands in our model. Most of the experimental states having molecular properties are assigned to these bands. The constancy of Q_0 is less pronounced for the $(\lambda,2)\chi=0$ bands, while it has a less regular, staggering character for the $(\lambda,1)1$ and $(\lambda,2)\chi=2$ bands. This is similar to the results for the 1^+ and 1^- bands in Ref. [13].

2. *E1 transitions*

In the present version of the model the phenomenologic electric dipole transition operator $T^{(E1)}$ contains only terms acting on the relative motion component of the wave function in Eq. (7). The usual first-order dipole operator, $D^{(1)}$ [11], is not enough for the sufficient description of $E1$ transitions in the ^{18}O nucleus, because its selection rules are too restrictive. It can generate only transitions with $\Delta n_\pi=\pm 1$, $\Delta\lambda=\pm 1$, $\Delta\mu=0$ and $\Delta n_\pi=\pm 1$, $\Delta\lambda=0$, $\Delta\mu=\mp 1$, the latter ones being much weaker. It is also unable to connect states with $\Delta n_\pi=\pm 3$, although our model should be able to describe transitions of this kind. Therefore, we also considered a third-order term in $T^{(E1)}$ to solve this problem:

$$T_m^{(E1)}=d_R D_m^{(1)}+f_R[D^{(1)}\times P^{(2)}+P^{(2)}\times D^{(1)}]_m^{(1)} \ . \qquad (13)$$

The most important selection rule of the second term is $\Delta n_\pi=\pm 3$, $\Delta\lambda=\pm 3$, $\Delta\mu=0$. Weaker transitions with $\Delta n_\pi=\pm 3$, $\Delta\lambda=\pm 2$, $\Delta\mu=\mp 1$ and even weaker ones with $\Delta\lambda=\pm 1$, $\Delta\mu=\mp 2$ are also allowed, but there are no examples for these within the present model basis (see Table I). The $\Delta n_\pi=\pm 1$ selection rules are also relaxed somewhat due to the presence of the second term in $T^{(E1)}$, and weak transitions with $\Delta n_\pi=\pm 1$, $\Delta\lambda=\pm 2$, $\Delta\mu=\pm 1$ and $\Delta n_\pi=\pm 1$, $\Delta\lambda=\mp 1$, $\Delta\mu=\mp 2$ also become possible.

We displayed our results and the experimental data [18,19] in Table III. We also presented the $B(E1)$ values obtained from an earlier GCM [13] and CCOCM [14] calculation. Certain selected enhanced $E1$ transitions were interpreted recently in terms of the simple vibron model [19]. Despite the similar formalism, this approach is essentially different from ours, e.g., it has a completely different model basis, nevertheless we displayed the results of Ref. [19] obtained in the U(3) dynamical symmetry case.

We fixed the two model parameters by requiring the reproduction of the two experimental $B(E1)$ values with the smallest relative error. The numerical values of the parameters obtained this way are $d_R=1.12$ and $f_R=-0.011$. (A least-squares fit of the model parameters using the inverse of the relative error as a weight for each transition amplitude resulted in similar values of d_R

and f_R.) The agreement between calculated and experimental values is much less satisfactory than in the $E2$ case. While the average magnitude of the theoretical and experimental $B(E1)$ values is similar, the intensity of some transitions is too small. Our model gives relatively strong $E1$ transitions between bands with the same μ, nevertheless all other transitions seem to be underestimated significantly. This is the result of the too strict selection rules of the phenomenologic $T^{(E1)}$ operator. These effects would probably be less pronounced if the SU(3) dynamical symmetry was broken, and the wave functions were a mixture of the basis states in Eq. (7).

Another difficulty is that experimental $B(E1)$ values for different transitions between the same bands usually

TABLE III. Reduced $E1$ transition probabilities (in 10^{-3} W.u.) between ^{18}O states. The more recent experimental compilation in Ref. [19] was used, whenever it was possible. Otherwise data were taken from Ref. [18], as indicated below. (E_x is given in units of MeV.)

Experimental data			$B(E1)$theory			Present work		
$J_i^\pi(E_{xi})$	$J_f^\pi(E_{xf})$	$B(E1)_{\text{exp}}$	[13]	[14]	[19]	$B(E1)$	$n_\pi(\lambda,\mu)\chi;i\rightarrow f$	
$1^-(4.46)$	$0^+(0.0)$	$<5.0\times10^{-4}$	28			5.7	7(5,0)0	6(4,0)0
	$2^+(1.98)$	0.40±0.10	40			9.8		6(4,0)0
	$0^+(3.63)$	28±7	63	56	28	5.7		8(6,0)0
	$2^+(3.92)$	3.7±1.7				0		8(8,2)2
$3^-(5.10)$	$2^+(1.98)$	0.57±0.23	23			6.9		6(4,0)0
	$4^+(3.55)$	0.37±0.17	11			5.3		6(4,0)0
	$2^+(3.92)$	2.5±1.0				0		8(8,2)2
$5^-(8.13)$	$4^+(3.55)$	6.1±1.1[a]	8			6.1[b]		6(4,0)0
	$4^+(7.12)$			170		3.7		8(6,0)0
$1^-(6.20)$	$0^+(0.0)$	1.6±0.3	1.1			0.1	7(6,1)1	6(4,0)0
	$2^+(1.98)$	0.056	1.8			0.02		6(4,0)0
	$0^+(3.63)$	0.64±0.13	29			0.2		8(6,0)0
	$2^+(5.26)$	18±3.3	52		12	0.02		8(6,0)0
	$0^+(5.34)$	7.4±2.4			15	0.02		8(8,2)0
	$2^+(3.92)$	<0.25				0.1		8(8,2)2
$2^+(5.26)$	$1^-(4.46)$	7.4±0.9	84	59	36	7.4[b]	8(6,0)0	7(5,0)0
	$3^-(5.10)$		73	67		8.3		7(5,0)0
$4^+(7.12)$	$3^-(5.10)$	0.31±0.08	74	180		7.8		7(5,0)0
	$3^-(6.40)$	<1.2				0		9(9,2)2
$6^+(11.69)$	$5^-(8.13)$			140		7.2		7(5,0)0
	$5^-(11.62)$			77		3.3		9(7,0)0
$2^+(8.21)$	$1^-(4.46)$	4.9±1.6[a]	13			0.1	8(7,1)1	7(5,0)0
	$3^-(5,10)$	5.0±1.1[a]	30			0.01		7(5,0)0
$4^+(10.29)$	$3^-(5.10)$		22	26		0.04		7(5,0)0
	$5^-(8.13)$		21	36		0.01		7(5,0)0
	$3^-(8.29)$		116	79		0.3		9(7,0)0
$0^+(5.34)$	$1^-(4.46)$	5.1±1.2			39	0	8(8,2)0	7(5,0)0
$6^+(12.53)$	$5^-(8.13)$			55		0	8(8,2)2	7(5,0)0
	$5^-(11.62)$			93		0		9(7,0)0
$1^-(7.62)$	$0^+(0.0)$	0.46±0.11[a]				3.7	9(7,0)0	6(4,0)0
	$2^+(1.98)$	$E1+M2$[a]				4.2		6(4,0)0
	$0^+(5.34)$	4.5±1.3[a]				0		8(8,2)0
$3^-(8.28)$	$2^+(1.98)$		1.4			4.9		6(4,0)0
	$4^+(3.55)$	6.1±1.6[a]	0.5			1.5		6(4,0)0
	$2^+(5.26)$	14±5[a]	94	78		8.8		8(6,0)0
	$4^+(7.12)$		111	35		7.2		8(6,0)0
$5^-(11.62)$	$4^+(7.12)$			52		9.2		8(6,0)0
	$4^+(10.29)$			84		0.1		8(7,1)1
$1^-(8.04)$	$0^+(0.0)$	0.70±0.17[a]				0	9(8,1)1	6(4,0)0
	$2^+(1.98)$	7.2±1.5[a]				0		6(4,0)0
	$0^+(3.63)$	0.28±0.08[a]				0.03		8(6,0)0
	$2^+(5.26)$	4.3±1.4[a]				0.01		8(6,0)0
$3^-(6.40)$	$2^+(1.98)$	0.37±0.19				0	9(9,2)0	6(4,0)0
	$4^+(3.55)$	0.15±0.08				0		6(4,0)0
	$2^+(5.26)$	1.8±0.9			28	0		8(6,0)0
	$2^+(3.92)$	0.19±0.10				5.1		8(8,2)2
$5^-(7.86)$	$4^+(3.55)$	>0.9[a]				0		6(4,0)0

[a]From Ref. [18].
[b]Used to fit model parameters.

differ by more than an order of magnitude, while model calculations give a more or less uniform set of amplitudes for such transitions. The most striking example for this is the set of $E1$ transitions between the 0_1^- and the 0_1^+ (ground-state) band. The extremely weak $1^-(4.46) \rightarrow 0^+(0.0)$ transition together with three more ones with $B(E1) \simeq 0.5 \times 10^{-3}$ W.u. cannot be reproduced either by our model or by other cluster studies [13,14]; rather all three models have $B(E1)$ values comparable to (or even larger than) that of the $5^-(8.13) \rightarrow 4^+(3.55)$ transition $[(6.1 \pm 1.1) \times 10^{-3}$ W.u.]. This fact suggests that the molecular component is overestimated in the wave functions of the lowest-lying states. In our case this arises from the fact that the $6(4,0)0^+$ ground-state band is very similar to the other bands with $(\lambda,0)$ SU(3) labels. Hence the matrix elements of the phenomenologic transition operators between the $(\lambda,0)$ and $(\lambda \pm 1,0)$ states are not expected to differ significantly for different values of λ. The $B(E1)$ values of transitions between the $K^\pi = 0_2^+$ band and the negative parity $K^\pi = 0_1^-$ and 0_2^- bands [which are labeled as $8(6,0)0^+$, $7(5,0)0^-$, and $9(7,0)^-$ in our approach] are relatively well reproduced, but the smaller $B(E1)$ observed for the $4^+(7.12) \rightarrow 3^-(5.10)$ transition is overestimated considerably (similarly to other model calculations).

Transitions to the ground-state band from higher-lying negative-parity states (assigned to $n_\pi = 9$ in our model) are reasonably well reproduced. $B(E1)$ values comparable to the experimental values were obtained for the $9(7,0)0^- \rightarrow 6(4,0)0^+ (K^\pi = 0_2^- \rightarrow 0_1^+)$ transitions. All other transitions with $\Delta n_\pi = -3$ are forbidden in the model, which seems to agree with the experimental situation, since most of these $B(E1)$ values are very small.

The microscopic cluster studies usually predict strong electric dipole transitions, which often exceed the experimental values by more than an order of magnitude. If we compare, however, the relative strength of transitions from a given band to various bands, we find that the GCM results [13] follow selection rules resembling those discussed earlier in this section. In particular, transitions to which we associate a significant change of the SU(3) labels λ and μ are usually weaker in the GCM description too. [See, for example, transitions from the $K^\pi = 1^-, 1^+$, and 0_2^- bands corresponding to $7(6,1)1^-$, $8(7,1)1^+$, and $9(7,0)0^-$ in our approach.] This again seems to suggest that some microscopic effects are approximated relatively well by combining the microscopic basis with phenomenologic operators within our semimicroscopic algebraic model.

The $B(E1)$ values obtained with the simple vibron model of [19] were calculated by applying the same phenomenologic dipole operator $D^{(1)}$ which we used in Eq. (13). Although the internal degrees of freedom of the clusters were ignored in this simple application (consequently, the model basis and the labeling of the experimental states was completely different from ours), the enhanced $E1$ transitions could be explained in a straightforward way [19]. In our interpretation, however, the four lowest-lying members of the mixed parity dipole band proposed by the authors [8,19] belong to the $n_\pi(\lambda,\mu)\chi^\pi = 8(6,0)0^+$, $7(5,0)0^-$, $8(6,0)0^+$, and $9(7,0)0^-$ bands, which are also connected by relatively strong $E1$ (and $E2$) transitions.

IV. SUMMARY AND CONCLUSIONS

In this paper we have applied a new semimicroscopic algebraic cluster model to the ^{18}O nucleus. The (0,2) SU(3) shell model representation was used to describe the internal structure of the ^{14}C nucleus. The model basis built on this ^{14}C configuration was found to be similar to that applied in microscopic cluster studies.

We restricted our calculations to the SU(3) dynamical symmetry limit, which allowed the analytic solution of the eigenvalue problem. We identified 34 $T = 1$ states of the experimental spectrum with model states and assigned them to 11 bands with both positive and negative parity. Several of these are new ones, while the others are essentially identical to cluster bands identified earlier. We were able to interpret almost every experimental state below $E_x = 10$ MeV in terms of our model.

Reduced $E2$ and $E1$ transition probabilities were also calculated applying phenomenologic transition operators. $E2$ transitions are generally in good agreement with the experimental data set (of 16 items); moreover, the quadrupole momentum of the first excited (2^+) state is also excellently reproduced. The results were somewhat poorer for the $E1$ transitions (30 items), mainly because of the too strict selection rules of the phenomenologic transition operators. It seems that by introducing symmetry breaking terms in the Hamiltonian more realistic results could be obtained.

A remarkable finding was that our results, especially the $B(E2)$ values, showed non-negligible correlation with the GCM results, in the sense that the same transitions were found strong (or weak) in the two models, sometimes even in contradiction to the experimental data. This trend was less pronounced for $E1$ transitions, but could be seen in the relative strength of transitions going form a given band to different bands. These results show that the semimicroscopic algebraic cluster model approximates certain microscopic effects reasonably well.

The well-known cluster states of the ^{18}O nucleus were assigned to model states belonging to the SU(3) representation labeled with $(\lambda,0)$ in our approach. These states have strong rotational character in our model and are connected by relatively strong $E2$ and $E1$ transitions. This is in accordance with their interpretation as states with molecular nature. $K^\pi = 1^+$ and 1^- bands were also reproduced; furthermore, two new bands based on the $2^+(3.92$ MeV) and the $2^-(5.53$ MeV) states were predicted. The proposed members of these bands are less well known experimentally. The few electromagnetic transitions to and from these states are generally weak, which is in accordance with our model calculations showing that these two bands are weakly connected by electromagnetic transitions to the $K^\pi = 1^+$ and 1^- bands, while transitions between them and the molecular bands discussed above are forbidden.

The semimicroscopic algebraic cluster model is able to reproduce several important characteristics of the ^{18}O nucleus. Furthermore, some results obtained from the

model, e.g., band structure, and the trend of reduced transition probabilities are similar to the corresponding results of microscopic cluster studies, which seem to indicate that the semimicroscopic model is able to account for some microscopic effects as, e.g., the antisymmetrization. The importance of this finding lies in the fact that although calculations get more involved for more complex nuclei, the semimicroscopic model can be applied to nuclear systems which may not be described by microscopic cluster models due to computational difficulties.

This work was supported by the DAAD, the Alexander von Humboldt Stiftung, and the OTKA (Grant No. 3008).

[1] F. Ajzenberg-Selove, Nucl. Phys. **A392**, 1 (1983).
[2] B. Buck, H. Friedrich, and A. A. Pilt, Nucl. Phys. **A290**, 205 (1977).
[3] T. Sakuda, Prog. Theor. Phys. **57**, 855 (1977).
[4] T. Sakuda, S. Nagata, and F. Nemoto, Prog. Theor. Phys. **59**, 1543 (1978).
[5] F. Iachello, Phys. Rev. C **23**, 2778 (1981).
[6] F. Iachello and A. D. Jackson, Phys. Lett. **108B**, 151 (1982).
[7] F. Iachello, Phys. Lett. **160B**, 1 (1985).
[8] M. Gai, M. Ruscev, A. C. Hayes, J. F. Ennis, R. Keddy, E. C. Schloemer, S. M. Sterbenz, and D. A. Bromley, Phys. Rev. Lett. **50**, 239 (1983).
[9] Y. Alhassid, M. Gai, and G. F. Bertsch, Phys. Rev. Lett. **49**, 1482 (1982).
[10] H. J. Assenbaum, K. Langanke, and A. Weiguny, Z. Phys. A **318**, 35 (1984).
[11] F. Iachello and R. D. Levine, J. Chem. Phys. **77**, 3046 (1982).
[12] D. Baye and P. Descouvemont, Phys. Lett. **146B**, 285 (1984).
[13] P. Descouvemont and D. Baye, Phys. Rev. C **31**, 2274 (1985).
[14] Y. Suzuki, A. Yamamoto, and K. Ikeda, Nucl. Phys. **A444**, 365 (1985).
[15] J. Cseh, Proceedings of the International Conference on Nuclear and Atomic Clusters, Turku 1991, Invited Papers (Springer, Berlin, in press).
[16] J. Cseh, Phys. Lett. B **281**, 173 (1992).
[17] J. P. Elliott, Proc. R. Soc. London Ser. A **245**, 128 (1958); **245**, 562 (1958).
[18] F. Ajzenberg-Selove, Nucl. Phys. **A475**, 1 (1987).
[19] M. Gai, M. Ruscev, D. A. Bromley, and J. W. Olnes, Phys. Rev. C **43**, 2127 (1991).
[20] M. Harvey, Adv. Nucl. Phys. **1**, 67 (1968).
[21] E. P. Wigner, Phys. Rev. **51**, 106 (1937).
[22] J. Cseh and G. Lévai, Phys. Rev. C **38**, 972 (1988).
[23] J. Cseh, J. Phys. Soc. Jpn. Suppl. **58**, 604 (1989).
[24] Y. Akiyama and J. P. Draayer, Comput. Phys. Commun. **5**, 405 (1973); J. P. Draayer and Y. Akiyama, J. Math. Phys. **14**, 1904 (1973).
[25] J. D. Vergados, Nucl Phys. **A111**, 681 (1968).
[26] J. Cseh, G. Lévai, and K. Katō, Phys. Rev. C **43**, 165 (1991).
[27] G. Lévai and J. Cseh, Phys. Rev. C **44**, 166 (1991).
[28] O. Castaños, J. P. Draayer, and Y. Leschber, Z. Phys. A **329**, 33 (1988).
[29] H. A. Naqvi and J. P. Draayer, Nucl. Phys. **A516**, 351 (1990).
[30] B. Buck, in *Proceedings of the 4th International Conference on Clustering Aspects of Nuclear Structure and Nuclear Reactions, Chester 1984,* Invited Papers, edited by J. S. Lilley and M. A. Nagarajan (Reidel, Dordrecht, 1985), p. 71.
[31] G. Lévai and J. Cseh, Phys. Rev. C **44**, 152 (1991).
[32] A. Bohr and B. R. Mottelson, *Nuclear Structure* (Benjamin, Massachusetts, 1975), Vol. 2.